

1 **The P681H mutation in the Spike glycoprotein confers Type I interferon**  
2 **resistance in the SARS-CoV-2 alpha (B.1.1.7) variant**

3 Maria Jose Lista<sup>1,4\*</sup>, Helena Winstone<sup>1,4\*</sup>, Harry D Wilson<sup>1,4</sup>, Adam Dyer<sup>1,4</sup>, Suzanne  
4 Pickering<sup>1,4</sup>, Rui Pedro Galao<sup>1,4</sup>, Giuditta De Lorenzo<sup>2</sup>, Vanessa M. Cowton<sup>2</sup>,  
5 Wilhelm Furnon<sup>2</sup>, Nicolas Suarez<sup>2</sup>, Richard Orton<sup>2</sup>, Massimo Palmarini<sup>2,4</sup>, Arvind H.  
6 Patel<sup>2,4</sup>, Luke Snell<sup>3</sup>, Gaia Nebbia<sup>3</sup>, Chad Swanson<sup>1</sup>, Stuart J D Neil<sup>1,4</sup>

7

8 \*These authors contributed equally to this work

9 1 Department of Infectious Diseases, King's College London

10 2 MRC-University of Glasgow Centre for Virus Research

11 3 Centre for Clinical Infection and Diagnostics Research, Department of Infectious  
12 Diseases, Guy's and St Thomas' NHS Foundation Trust

13 4 UKRI Gentotype-2-Phenotype consortium

14

15 Corresponding author:

16 Stuart Neil

17 Email: [stuart.neil@kcl.ac.uk](mailto:stuart.neil@kcl.ac.uk)

18

19

20 **SUMMARY**

21 **Variants of concern (VOCs) of severe acute respiratory syndrome coronavirus**  
22 **type-2 (SARS-CoV-2) threaten the global response to the COVID-19 pandemic.**  
23 **The alpha (B.1.1.7) variant appeared in the UK became dominant in Europe and**  
24 **North America in early 2021. The Spike glycoprotein of alpha has acquired a**  
25 **number mutations including the P681H mutation in the polybasic cleavage site**  
26 **that has been suggested to enhance Spike cleavage. Here, we show that the**  
27 **alpha Spike protein confers a level of resistance to the effects of interferon- $\beta$**   
28 **(IFN $\beta$ ) in lung epithelial cells. This correlates with resistance to restriction**  
29 **mediated by interferon-induced transmembrane protein-2 (IFITM2) and a**  
30 **pronounced infection enhancement by IFITM3. Furthermore, the P681H**  
31 **mutation is necessary for comparative resistance to IFN $\beta$  in a molecularly**  
32 **cloned SARS-CoV-2 encoding alpha Spike. Overall, we suggest that in**  
33 **addition to adaptive immune escape, mutations associated with VOCs also**  
34 **confer replication advantage through adaptation to resist innate immunity.**

35

36

37

## 38 INTRODUCTION

39 Both SARS-CoV-1 and SARS-CoV-2 enter target cells through the interaction of their  
40 Spike proteins with the angiotensin converting enzyme 2 (ACE2) cell surface  
41 receptor. Upon attachment and uptake, the Spike glycoprotein trimer is cleaved by  
42 cellular proteases such as cathepsins and TMPRSS family members at two positions  
43 – the S1/S2 junction and the S2' site – to facilitate the activation of the fusion  
44 mechanism. Similar to more distantly related beta-CoVs, but so far unique in known  
45 Sarbecoviruses, the SARS-CoV-2 glycoprotein contains a polybasic furin cleavage  
46 site (FCS) with a (681-PRRAR-685) sequence at the S1/S2 junction. This allows the  
47 Spike precursor to be processed to the S1 and S2 subunits by furin-like proteases  
48 before viral release from the previously infected cell (Hoffmann et al., 2020). This  
49 leads to a proportion of processed Spikes to be present on the virion before  
50 engagement with the target cell, allowing for rapid activation and fusion at or near  
51 the cell surface by TMPRSS2. The importance of the FCS is highlighted by the  
52 observations that it enhances SARS-CoV-2 replication specifically in airway epithelial  
53 cells and is essential for efficient transmission in animal models (Peacock et al.,  
54 2021a).

55

56 The alpha variant of SARS-CoV-2 arose in the South-East of England in autumn  
57 2020, and rapidly spread across the world in the first months of 2021. Various  
58 studies suggested that alpha had an increased transmissibility between  
59 individuals (Lindstrom et al., 2021; Mok et al., 2021; Tanaka et al., 2021). Alpha  
60 contains nine amino acid residue changes in Spike including a deletion of amino acid  
61 residues H and V in the N-terminal domain at position 69/70, thought to increase  
62 Spike incorporation into virions, a single amino acid deletion of Y144 (thought to

63 assist NTD antibody neutralization escape), and a N501Y mutation in the RBD which  
64 enhances ACE2 binding affinity (Meng et al., 2021),(Chi et al., 2020). Together these  
65 changes have been shown to reduce efficiency of neutralization by some  
66 antibodies(Graham et al., 2021). Alpha also acquired a P681H change in the FCS  
67 which has been shown to increase the accessibility of the site by furin leading to  
68 enhanced cleavage(Mohammad et al., 2021),(Zhang et al., 2021). The alpha variant  
69 Spike has also recently been reported to mediate more efficient cell-to-cell fusion  
70 and syncytia formation (Michael Rajah et al., 2021),(Sanches et al., 2021).

71

72 We and others have previously found that SARS-CoV-2 is variably sensitive to entry  
73 inhibition by the interferon-regulated IFITM family (Winstone et al., 2021),(Shi et al.,  
74 2021). the three members of the family form multimeric complexes and have antiviral  
75 activity against diverse enveloped viruses by blocking fusion of the viral and cellular  
76 membranes (Bailey et al., 2014; Shi et al., 2017). While IFITM1 localizes primarily to  
77 the plasma membrane, IFITM2 and IFITM3 are internalized via a conserved YxxΦ  
78 endocytic motif to occupy distinct and overlapping endosomal compartments(Jia et  
79 al., 2012; Jia et al., 2014). The sensitivity of a given virus to individual IFITM proteins  
80 is largely determined by their route of cellular entry. We have previously shown that  
81 for a prototypic Wuhan-like SARS-CoV-2 isolate from early 2020, IFITM2 reduced  
82 viral entry and contributed to type I interferon (IFN-I)-induced inhibition in human  
83 cells(Winstone et al., 2021). Sensitivity to IFITM2 could be markedly enhanced by  
84 deletion of the FCS, suggesting that furin processing ameliorated SARS-CoV-2  
85 sensitivity to IFITM2-restriction at least to some extent. We therefore postulated that  
86 the altered cleavage site of alpha may have consequences for its sensitivity to IFN-I  
87 and IFITMs. Here, we demonstrate that the Spike of the alpha variant is less

88 sensitive to restriction by IFN $\beta$  and IFITMs in A549-ACE2 and Calu-3 cells.  
89 Furthermore, this resistance correlates with the enhanced polybasic site as reversion  
90 of this cleavage site increases the alpha variant's sensitivity to IFITM restriction.  
91 Finally, we demonstrate that the H681P reversion in the full-length virus confers  
92 IFN $\beta$  sensitivity to alpha and suggest that part of this phenotype is driven by IFITMs.

93

## 94 **RESULTS**

### 95 **The Spike proteins of currently circulating variants display differing** 96 **sensitivities to IFITMs in A549-ACE2 cells**

97 Previously we have shown that viral entry mediated by the original Wuhan-1 Spike  
98 pseudotyped lentiviral particle (PLV) or the England 02 isolate (hCoV-  
99 19/England/02/2020) was inhibited by IFITM2 in A549-ACE2 cells, and that this  
100 effect correlated in part with the IFN $\beta$  sensitivity of the virus(Winstone et al., 2021).  
101 Over 2020 and 2021 several major variants of concern (VOCs) have arisen – alpha  
102 (B.1.1.7) in the UK, beta (B.1.351) in South Africa, gamma (P1) in Brazil, and delta  
103 (B.1.617.2) in India. We wanted to compare the sensitivity of viral entry of the alpha,  
104 beta, gamma and delta to the presence of IFITM proteins, given that these variants  
105 have several changes in the Spike sequence (Figure 1A). Initially, PLVs bearing the  
106 spike protein of each variant to test whether they were restricted by IFITMs  
107 overexpressed on A549-ACE2 cells (Figure 1B-G). First, we confirmed that the  
108 D614G mutation in the parental Wuhan-1 Spike that became prevalent in the first  
109 wave of the pandemic displays a similar IFITM phenotype to the previously  
110 characterised SARS-CoV-2 Spike (Wuhan-1) (Figure 1B, 1C)(Winstone et al., 2021).  
111 The addition of D614G to the Wuhan-1 Spike had no effect on IFITM1 and IFITM2  
112 sensitivity of PLV entry, while we observe a slight enhancement in the presence of

113 IFITM3. We next compared the IFITM sensitivities of the major global VOCs. The  
114 alpha Spike appeared completely insensitive to IFITMs 1, 2 or 3 whilst beta, gamma  
115 and delta still retain some sensitivity to IFITMs 1 and/or 2 (Figure 1B-G). None of the  
116 VOCs were restricted by IFITM3 and, interestingly, we noted that IFITM3 appeared  
117 to markedly enhance entry mediated by the alpha variant Spike. Next, we pre-treated  
118 A549-ACE2-IFITM3 cells with cyclosporin H as this compound is known to drive  
119 IFITM3 to degradation (Petrillo et al., 2018), and showed that this led to a specific  
120 abolishment of the enhanced infection by alpha PLVs (Supplemental Figure 1).  
121 Henceforth, we selected alpha to further investigate and determine the mechanism  
122 of IFITM resistance.

123         Next, to confirm whether IFITM sensitivity results seen with the alpha spike  
124 PLVs could be recapitulated with the full-length virus (Figure 2A), we infected A549-  
125 ACE2 cells (stably expressing IFITMs or not) with either the Wuhan-like England/02  
126 isolate or alpha at an MOI of 0.01 and measured infection by qPCR of E copies in  
127 the infected cells 48 hours later (Figure 2B). As expected, replication of England/02  
128 was significantly reduced in IFITM2 expressing cells over 48h. By contrast alpha  
129 replicated as well in IFITM2-expressing cells and to a significantly higher level in  
130 IFITM3-expressing cells in comparison to the control A549-ACE2 cells. This  
131 confirmed that alpha SARS-CoV-2 is resistant to the effects of IFITMs 1 and 2 and  
132 enhanced by IFITM3 on viral entry. Previous reports have suggested that the alpha  
133 spike is more efficiently cleaved than Wuhan-like isolates due to the presence of the  
134 P681H mutation optimising the accessibility of the FCS (Mohammad et al., 2021;  
135 Zhang et al., 2021) We immunoblotted our viral stocks of England-02 and alpha and  
136 confirmed that the alpha has more processed spike on the virions (Figure 2C, right  
137 panel), although it was not as clearly discernible a difference in processing on PLVs

138 (Figure 2C, left panel). However, PLV infection in A549-ACE2 cells pre-treated with  
139 E64D, a cathepsin inhibitor, that inhibits the entry of SARS-CoV-2 in endosomal  
140 compartments because it cleaves S1/S2 junctions that have not been processed by  
141 furin. This showed that the alpha variant Spike mediated entry of PLVs is markedly  
142 less sensitive to this endosomal protease inhibition, when compared with the  
143 Wuhan-1/D614G Spike, indicating differences in the site of virus entry mediated  
144 consistent with enhanced Spike processing by furin in the producer cell  
145 (Supplementary Figure 2).

#### 146 **The alpha variant is less sensitive to IFN $\beta$ than a wave 1 isolate**

147 While previous data has indicated that the original Wuhan-like SARS-CoV-2 virus  
148 can delay pattern recognition of viral RNA in target cells, its replication highly  
149 sensitive to exogenous interferon treatment in culture, in part determined by  
150 IFITM2(Jouvenet, 2021). Having confirmed that the alpha variant is resistant to  
151 IFITMs expression when ectopically expressed in cells, we then tested if alpha is  
152 also resistant to the effects of IFN $\beta$ , as suggested(Guo et al., 2021; Thorne et al.,  
153 2021). Indeed, we found from measuring supernatant viral RNA 48 hours after  
154 infection of both A549-ACE2 cells and the human lung epithelial cell line Calu3,  
155 which more faithfully represent target cells in the respiratory tract, that alpha is more  
156 resistant than England/02 to pre-treatment with increasing doses of IFN $\beta$  (Figure 3A,  
157 3B). We have also confirmed this phenotype by measuring viral RNA in cell lysates,  
158 and further extending these observations to two clinical isolates of alpha isolated  
159 (clinical isolates 10 and 28; Figure 3C). Thus in comparison to a representative  
160 example of Wuhan-1-like SARS-CoV-2, the alpha variant has a marked resistance  
161 to type I interferon.

162 **The P681H mutation is necessary for conferring IFITM and IFN $\beta$  resistance in**  
163 **alpha**

164 Our previous data indicated IFITM sensitivity of SARS-CoV-2 Spike can be  
165 increased by deleting the FCS. Given that alpha and delta Spikes have acquired  
166 mutations at P681 to H or R respectively, and these enhance Spike cleavage to  
167 S1/S2 (Supplementary figure 3), we hypothesized that P681H might be a  
168 determinant of resistance to IFN and IFITM. First we confirmed that none of the other  
169 individual alpha-Spike defining mutations were sufficient to confer IFITM resistance  
170 to a Wuhan/D614G Spike in PLVs (Supplementary figure 4 A–F). By contrast a  
171 P681H mutation in the Wuhan-1/D614G Spike was sufficient to abolish IFITM2-  
172 mediated inhibition PLVs entry, but not to fully confer the IFITM3-mediated  
173 enhancement phenotype (Figure 4A). As expected, deletion of the HRRRA cleavage  
174 site in the alpha Spike conferred potent sensitivity to IFITM2 and reduced the level of  
175 enhancement we showed with IFITM3. Finally, we reverted the mutation in alpha to  
176 H681P and showed it gained IFITM2 sensitivity. Thus, the H681P mutation in the  
177 alpha spike confers IFITM resistance consistent with its enhanced furin cleavage.  
178 However delta bears a P681R mutation yet is not fully IFITM resistant (Figure 1G),  
179 implying that the P681H phenotype may be context dependent. Indeed, we found  
180 that combining the P681H mutation in the Wuhan spike with the deletion at position  
181 69-70 in the NTD found in the alpha variant but not delta was sufficient to fully confer  
182 an alpha spike phenotype to D614G (Supplementary figure 4G). This suggests that  
183 the H681 confers IFITM resistance in the context of other adaptations in the alpha  
184 Spike that are thought to affect the conformation of S1 and the interaction with  
185 ACE2.



186           Having established that P681H change is necessary for the resistance of the  
187 alpha variant Spike to IFITMs, we next wanted to address if this was also a  
188 determinant for the resistance to type-I IFN resistance of the virus itself. We  
189 constructed a recombinant molecular clone of SARS-CoV-2 Wuhan-1 encoding  
190 Spike from the alpha variant. This virus essentially mimicked the resistance of the  
191 alpha variant itself to IFN $\beta$  in comparison to a representative Wuhan-1 like virus,  
192 England-02, demonstrating that the alpha Spike alone is sufficient to confer a level  
193 type I IFN resistance in A549-ACE2 cells (Figure 4B). We then took this recombinant  
194 virus and reverted the amino acid residue H681 to a proline. Importantly, this single  
195 point mutation was sufficient to confer a significant sensitivity to IFN $\beta$  in Calu3 cells  
196 (Figure 4C). Lastly, we wanted to confirm whether siRNA knockdown of IFITM2 was  
197 sufficient to rescue the IFN sensitivity of the Wuhan(B.1.1.7 Spike H681P) virus. We  
198 therefore knocked down IFITM2 expression using siRNA in A549-ACE2 cells and  
199 treated the cells with IFN $\beta$  as before. We found that the H681P reverted virus was  
200 rescued from IFN $\beta$  restriction during IFITM2 knockdown, meanwhile the  
201 Wuhan(B.1.1.7 Spike) virus was unaffected, consistent with this virus being resistant  
202 to IFITM2 restriction. Thus, this confirmed that the Spike protein of the alpha variant  
203 of SARS-CoV-2 is a determinant of type-I IFN resistance and that the P681H  
204 mutation is necessary for this.

205

## 206 **DISCUSSION**

207 Here we have shown that the Spike protein of the alpha variant of SARS-CoV-2 is  
208 resistant to IFN-I. Furthermore, we show that this maps to the histidine residue  
209 adjacent to the FCS that has been mutated from the parental proline, which has  
210 been shown to enhance Spike cleavage at the S1/S2 boundary (Peacock et al.,

211 2021b). This residue is necessary to confer resistance to IFITM2 and enhancement  
212 by IFITM3, and as we demonstrated in our previous study(Winstone et al., 2021),  
213 confirms that the FCS in Spike modulates IFITM entry restriction. Changes in the  
214 FCS would be predicted to increase the efficiency of viral fusion and entry at or near  
215 the plasma membrane, avoiding endosomal compartments where IFITMs 2 and 3  
216 predominantly reside. Consistent with this, we show that the alpha Spike, as a PLV,  
217 is less sensitive to the cathepsin inhibitor E64D. Thus we propose that these  
218 changes in the alpha Spike have, in part, arisen to resist innate immunity.

219 At least two preprints suggest that variants of SARS-CoV-2 have begun to  
220 evolve further resistance to interferon-induced innate immunity (Guo et al., 2021;  
221 Thorne et al., 2021). In one, viral isolates over the pandemic show a reduced  
222 sensitivity to type I interferons in culture(Guo et al., 2021); in a second the alpha  
223 variant has a significantly reduced propensity to trigger pattern recognition in  
224 epithelial cells(Thorne et al., 2021). In contrast, another study shows no difference in  
225 IFN sensitivity of the new variants in African green monkey Vero-E6 cells(Michael  
226 Rajah et al., 2021), although species-specificity in viral sensitivity to ISGs is a well  
227 characterized trait. The SARS-CoV-2 genome contains multiple mechanisms to  
228 counteract host innate immune responses, and much remains to be learned about  
229 the mechanisms deployed by this virus and its relatives. While many reports on  
230 SARS-CoV-2 evolution have naturally focussed on the pressing concern of potential  
231 for vaccine escape, it is very unlikely that all selective adaptations that we see  
232 arising in VOCs can be solely due to escape from adaptive immunity. The alpha  
233 variant Spike, for example, only displays a minor reduction in sensitivity to  
234 neutralizing antibodies (NAbs) (Graham et al., 2021; Mahase, 2021; Planas et al.,  
235 2021; Shen et al., 2021). However, this VOC had a considerable transmission

236 advantage, with suspicions that it may have arisen in an immunocompromised  
237 individual with a persistent infection giving ample time for changes to be selected  
238 that further evade innate immunity, including those that target viral entry (Corey et al.,  
239 2021; Kemp et al., 2021).

240 In terms of IFITM resistance of VOC Spike proteins, so far we have only seen  
241 marked change in phenotype for the alpha variant. This is despite the fact that delta,  
242 which has superseded alpha in many places around the world in 2021, also shows  
243 an adaptation for enhanced S1/S2 cleavage with an P681R change (Liu et al., 2021;  
244 Peacock et al., 2021b). This would suggest that efficient cleavage of S1/S2 is  
245 necessary but not sufficient for IFITM resistance, and indeed our data implicate a  
246 context dependency of the NTD deletion at 69/70. While unique to the alpha VOC,  
247 the 69/70 deletion has been observed in persistent infection of immunosuppressed  
248 individuals and is thought to enhance viral fitness and Spike stability (Meng et al.,  
249 2021). While deletions in the NTD do affect NAb binding, it is primarily the 144  
250 deletion in the alpha Spike that escapes neutralization by NTD-directed Nabs (Chi et  
251 al., 2020) and we show that this has no impact on IFITM sensitivity. By contrast, the  
252 more pronounced antibody evasion by the beta, gamma and delta variants is related  
253 to mutations in the major neutralizing epitopes of the RBD, suggesting that they may  
254 well have been driven by antibody escape (Planas et al., 2021; Zhou et al., 2021).  
255 Viral glycoproteins are dynamic structures that shift through large-scale  
256 conformational changes while interacting with their cognate receptors mediating viral  
257 membrane fusion. Such context dependency is therefore likely to be complex and  
258 will arise under competing selective pressures. Indeed, we have previously shown  
259 that the HIV-1 envelope glycoprotein of transmitted viruses is IFITM insensitive and  
260 this contributes to their overall type I IFN resistance (Foster et al., 2016). As HIV-1

261 infection progresses over the first 6 months in an infected person, the circulating  
262 variants increase in IFN/IFITM sensitivity and this is determined by adaptive changes  
263 in Env that resist the early neutralizing antibody response (Fenton-May et al., 2013).  
264 Such escape has structural and functional implications for such dynamic proteins  
265 that may impact upon receptor interactions and route of entry into the target cell.

266         While furin cleavage of the SARS-CoV-2 Spike reduces its IFITM sensitivity,  
267 other interferon-induced proteins may contribute to this phenotype. The guanylate  
268 binding protein family, and particularly GBP2 and GBP5, have been shown to have a  
269 general antiviral activity against enveloped viruses by dysregulating furin processing  
270 of diverse viral and cellular proteins (Braun et al., 2019). Similarly, IFITM  
271 overexpression in HIV-infected cells can lead to their incorporation into virions and in  
272 some cases promote defects in glycoprotein incorporation (Tartour et al., 2014).  
273 Future studies will confirm whether either of these mechanisms are involved in the  
274 IFN-resistance associated with the P681H mutation in alpha.

275         In summary, the spike protein of SARS-CoV-2 alpha increases resistance to  
276 IFN-I and this correlates with the P681H mutation. Furthermore, this correlates with  
277 resistance to IFITM-mediated entry restriction. This suggests that in addition to  
278 adaptive immune escape, fixed mutations associated with VOCs may well also  
279 confer replication and/or transmission advantage through adaptation to resist innate  
280 immune mechanisms.

281

282

## 283 MATERIALS AND METHODS

### 284 Cells and plasmids

285 HEK293T-17 (ATCC, CRL-11268<sup>TM</sup>), Calu-3 (ATCC, HTB-55<sup>TM</sup>), A549-ACE2, Vero-  
286 E6, Vero-E6-TMPRSS2 and A549-ACE2 expressing the individual IFITM proteins  
287 were cultured in DMEM (Gibco) with 10% FBS (Invitrogen) and 200µg/ml Gentamicin  
288 (Sigma), and incubated at 37°C, 5% CO<sub>2</sub>. ACE2, TMPRSS2, and IFITM stable  
289 overexpression cells were generated as previously described (Winstone et al.,  
290 2021).

291 Codon optimised SARS-CoV-2 Wuhan Spike and ACE2 were kindly given by Dr.  
292 Nigel Temperton. Codon optimised variant Spikes (B.1.1.7, B.1.351) were kindly  
293 given by Dr. Katie Doores. Codon optimised variant Spikes (P1, B.617.2) were kindly  
294 given by Professor Wendy Barclay. Plasmid containing TMPRSS2 gene was kindly  
295 given by Dr. Caroline Goujon. Spike mutants were generated with Q5® Site-Directed  
296 Mutagenesis Kit (E0554) following the manufacturer's instructions, and using the  
297 following forward and reverse primers:

298 D614G (GCTGTACCAGGGCGTGAATTGCA, ACGGCCACCTGATTGCTG)

299 B.1.351. Δ242-244 (ATTTTCATATCTTACACCAGGC, ATGCAGGGTCTGGAATCTG)

300 D614G P681H (GACCAATAGCcacAGAAGAGCCAGAAGC,

301 TGGGTCTGGTAGCTGGCG)

302 B117 ΔHRRA (AGAAGCGTGGCCAGCCAG, GCTATTGGTCTGGGTCTGGTAG)

303 B117 H681P (GACCAATAGCcccAGAAGAGCCAG, TGGGTCTGGTAGCTGGCG)

304 Δ144 (CATAAGAACAACAAGAGC, ATAAACACCCAGGAAAGG), N501Y

305 (CCAGCCTACctacGGCGTGGGCT, AAGCCGTAGCTCTGCAGAG), E484K

306 (TAATGGCGTGAACGGCTTCAATTGCTACTT, CACGGTGTGCTGCCGGCC).

307 A549 stable cell lines expressing ACE2 (pMIGR1-puro), and IFITMs (pLHCX) were  
308 generated and selected as described previously (Winstone et al., 2021).

### 309 **Production of Pseudotyped Lentiviral Vectors (PLVs) and infection**

310 HEK293T-17 were transfected with firefly luciferase expressing vector (CSXW), HIV  
311 gag-pol (8.91) and Spike plasmid with PEI-max as previously described (Winstone et  
312 al., 2021). Viral supernatant was then used to transduce each cell line of interest and  
313 readout measured by Luciferase activity 48 hours later (Promega Steady-Glo®  
314 (E2550)).

### 315 **Cyclosporin H assay**

316 Cells were pre-treated with 30µM of Cyclosporin H (Sigma, SML1575) for 18 hours.  
317 Cells were then infected with PLVs and viral entry quantified by Luciferase activity 48  
318 hours later.

### 319 **Passage and titration of SARS-CoV-2**

320 PHE England strain 02/2020 was propagated in Vero-E6-TMPRSS2 cells and titre  
321 was determined by plaque assay (Winstone et al., 2021). Vero-E6-TMPRSS2 were  
322 infected with serial dilutions of SARS-CoV-2 for 1h. Subsequently, 2X overlay media  
323 (DMEM + 2% FBS + 0.1% agarose) was added, and infected cells were fixed 72  
324 hours after infection and stained with Crystal Violet. Plaques were counted and  
325 multiplicity of infection calculated for subsequent experiments. A replication-  
326 competent alpha variant was kindly provided by Professor Wendy Barclay (Imperial  
327 College London)(Brown et al., 2021). All virus stocks were sequence confirmed in  
328 the Spike gene at each passage to ensure no loss of the FCS.

### 329 **Generation of recombinant full-length viruses**

330 We used the previously described Transformation-Associated Recombination  
331 (TAR) in yeast method(Thi Nhu Thao et al., 2020), with some modifications, to  
332 generate the mutant viruses described in this study. Briefly, a set of overlapping  
333 cDNA fragments representing the entire genomes of SARS-CoV-2 Wuhan isolate  
334 (GenBank: MN908947.3) and the B.1.1.7 alpha variant were chemically synthesized  
335 and cloned into pUC57-Kan (Bio Basic Canada Inc and Genewiz, respectively). The  
336 cDNA fragment representing the 5' terminus of the viral genome contained the  
337 bacteriophage T7 RNA polymerase promoter preceded by a short sequence stretch  
338 homologous to the *XhoI*-cut end of the TAR in yeast vector pEB2(Gaida et al., 2011).  
339 The fragment representing the 3' terminus contained the T7 RNA polymerase  
340 termination sequences followed by a short segment homologous to the *BamHI*-cut  
341 end of pEB2.

342 To generate Wuhan virus carrying the alpha variant spike, a mixture of the  
343 relevant synthetic cDNA fragments of the Wuhan and alpha variants was co-  
344 transformed with *XhoI*-*BamHI*-cut pEB2 into the *Saccharomyces cerevisiae* strain  
345 TYC1 (MATa, ura3-52, leu2 $\Delta$ 1, cyh2<sup>r</sup>, containing a knockout of DNA Ligase 4)  
346 (Gaida et al., 2011) that had been made competent for DNA uptake using the LiCl<sub>2</sub>-  
347 based Yeast transformation kit (YEAST1-1KT, Merck). The transformed cells were  
348 plated on minimal synthetic defined (SD) agar medium lacking uracil (Ura) but  
349 containing 0.002% (w/v) cycloheximide to prevent selection of cells carrying the  
350 empty vector. Following incubation at 30°C for 4 to 5 days, colonies of the yeast  
351 transformants were screened by PCR using specific primers to identify those  
352 carrying plasmid with fully assembled genomes. Selected positive colonies were  
353 then expanded to grow in 200 ml SD-Ura dropout medium and the plasmid  
354 extracted. Approximately 4  $\mu$ g of the extracted material was then used as template to

355 *in vitro* synthesized viral genomic RNA transcripts using the Ribomax T7 RNA  
356 transcription Kit (Promega) and Ribo m7G Cap Analogue (Promega) as per the  
357 manufacturer's protocol. Approximately 2.5 µg of the *in vitro* synthesized RNA was  
358 used to transfect ~6 x10<sup>5</sup> BHK-hACE2-N cells stably expressing the SARS-CoV-2 N  
359 and the human ACE2 genes(Rihn et al., 2021) using the MessengerMax lipofection  
360 kit (Thermo Scientific) as per the manufacturer's instructions. Cells were then  
361 incubated until signs of viral replication (syncytia formation) became visible (usually  
362 after 2-3 days), at which time the medium was collected (P0 stock) and used further  
363 as a source of rescued virus to infect VERO E6 cells to generate P1 and P2 stocks.  
364 Full genome sequences of viruses collected from from P0 and P1 stocks were  
365 obtained in order to confirm the presence of the desired mutations and exclude the  
366 presence of other spurious mutations. Viruses were sequenced using Oxford  
367 Nanopore as previously described(da Silva Filipe et al., 2021).

368 To generate Wuhan virus carrying alpha spike gene with the H681P mutation,  
369 we first introduced this mutation into the relevant alpha variant cDNA fragment by  
370 site-directed mutagenesis. This fragment was combined with those described above  
371 and the mixture was then used to generate plasmid pEB2 carrying the cDNA  
372 genome of Wuhan encoding the alpha spike H681P by the TAR in yeast procedure.  
373 The virus rescue and subsequent characterisation were performed as described  
374 above.

### 375 **Generation of Clinical Viral Isolates**

376 Viruses were isolated on Vero.E6 cells (ATCC CRL 1586™) from combined naso-  
377 oropharyngeal swabs submitted for routine diagnostic testing by real-time RT-PCR  
378 and shown to be from the B.1.1.7 (alpha) variant by on-site whole-genome  
379 sequencing (Oxford Nanopore Technologies, Oxford, UK) (Pickering et al., 2021).



380 Infected cells were cultured at 37°C and 5% CO<sub>2</sub>, in Dulbecco's modified Eagle's  
381 medium (DMEM, Gibco™, Thermo Fisher, UK) supplemented with 2% foetal bovine  
382 serum (FBS, Merck, Germany), pen/strep and amphotericin B.

383 All work performed with full-length SARS-CoV-2 preparations, as well as isolation  
384 and propagation of viral isolates from swabs, was conducted inside a class II  
385 microbiological safety cabinet in a biosafety level 3 (BSL3) facility at King's College  
386 London.

### 387 **Infection with replication competent SARS-CoV-2**

388  $1.5 \times 10^5$  A549-ACE2 cells were infected for 1 hour at 37°C with SARS-CoV-2  
389 replication competent viruses at MOI 0.01 or 500 E gene mRNA copies/cell.  $2 \times 10^5$   
390 Calu-3 cells were infected for 1h at 37°C with SARS-CoV-2 replication competent  
391 viruses at 5000 copies/cell. Media was replaced and cells were incubated for 48  
392 hours at 37°C, after which cells or supernatant were harvested for RNA extraction or  
393 protein analysis.

### 394 **Interferon assays**

395 Cells were treated with different doses of IFN $\beta$  (PBL Assay Science, 11415-1) for 18  
396 hours prior infection. The following day media was replaced, and the infection  
397 performed as described above. Viral RNA levels in cells or supernatants were  
398 measured 48 hours after infection by RT-qPCR .

### 399 **siRNA knockdown of IFITM2**

400 A549-ACE2 cells were reverse transfected using 20pmol of Non-targeting siRNA (D-  
401 001206-13-20) or IFITM2 siRNA (M-020103-02-0010) and 1 $\mu$ L of RNAi max  
402 (Invitrogen). Cells were incubated for 24h prior to a second round of reverse

403 transfection. 8h later, cells were treated with different doses of IFN $\beta$ . Following 18h  
404 of IFN treatment cells were infected with full-length viruses as previously described.

#### 405 **RT-qPCR**

406 RNA from infected cells was extracted using QIAGEN RNeasy (QIAGEN RNeasy  
407 Mini Kit, 74106) following the manufacturer's instructions. 1 $\mu$ L of each extracted  
408 RNA was used to performed one step RT-qPCR using TaqMan Fast Virus 1-Step  
409 Master Mix (Invitrogen). The relative quantities of envelope (E) gene were measured  
410 using SARS-CoV-2 (2019-nCoV) CDC qPCR Probe Assay (IDT DNA technologies).  
411 Relative quantities of E gene were normalised to GAPDH mRNA levels (Applied  
412 Bioscience, Hs99999905\_m1).

413 Supernatant RNA was extracted using RNAAdvance Viral XP (Beckman) following the  
414 manufacturer's instructions. 5 $\mu$ L of each RNA was used for one-step RT-qPCR  
415 (TaqMan<sup>TM</sup> Fast Virus 1-Step Master Mix) to measured relative quantities of E and  
416 calibrated to a standard curve of E kindly provided by Professor Wendy Barclay.

#### 417 **SDS-PAGE and Western blotting**

418 Cellular samples were lysed in reducing Laemmli buffer at 95 $^{\circ}$ C for 10 minutes.  
419 Supernatant or viral stock samples were centrifuged at 18,000 RCF through a 20%  
420 sucrose cushion for 1 hour at 4 $^{\circ}$ C prior to lysis in reducing Laemmli buffer. Samples  
421 were separated on 8–16 % Mini-PROTEAN<sup>®</sup> TGX<sup>TM</sup> Precast gels (Bio-Rad) and  
422 transferred onto nitrocellulose membrane. Membranes were blocked in milk prior to  
423 detection with specific antibodies: 1:1000 ACE2 rabbit (Abcam, Ab108209), 1:5000  
424 GAPDH rabbit (Abcam, Ab9485), 1:5000 HSP90 mouse (Genetex, Gtx109753), 1:50  
425 HIV-1 p24Gag mouse (48 ref before) 1:1000 Spike mouse (Genetex, Gtx632604),

426 1:1000 anti-SARS-CoV-2 N rabbit (GeneTex, GTX135357). Proteins were detected  
427 using LI-COR and ImageQuant LAS 4000 cameras.

#### 428 **Ethics**

429 Clinical samples were retrieved by the direct care team in the Directorate of  
430 Infection, at St Thomas Hospital, London, UK, and anonymised before sending to the  
431 King's College London laboratories for virus isolation and propagation. Sample  
432 collection and studies were performed in accordance with the UK Policy Framework  
433 for Health and Social Care Research and with specific Research Ethics Committee  
434 approval (REC 20/SC/0310).

#### 435 **ACKNOWLEDGEMENTS**

436 We are grateful to Nigel Temperton, Caroline Goujon, Katie Doores, Wendy Barclay  
437 and Public Health England for reagents. We acknowledge the G2P-UK National  
438 Virology consortium funded by MRC/UKRI (grant ref: MR/W005611/1) and the  
439 Barclay Lab at Imperial College London for providing the alpha variant. We thank E.  
440 J. Louis, University of Leicester for generously providing the TAR in yeast system.

#### 441 **FUNDING**

442 This work was funded by Wellcome Trust Senior Research Fellowship  
443 WT098049AIA to SJDN, MRC Project Grant MR/S000844/1 to SJDN and CMS, and  
444 funding from the Huo Family Foundation jointly to SJDN, Katie Doores, Michael  
445 Malim and Rocio Martinez Nunez. MR/S000844/1 is part of the EDCTP2 programme  
446 supported by the European Union. HW is supported by the UK Medical Research  
447 Council (MR/N013700/1) and is a King's College London member of the MRC  
448 Doctoral Training Partnership in Biomedical Sciences. This work is supported by the  
449 UKRI SARS-CoV-2 Genotype-2-Phenotype consortium. We also benefit from  
450 infrastructure support from the KCL Biomedical Research Centre, King's Health

451 Partners. Work at the CVR was also supported by the MRC MC\_UU12014/2 and the  
452 Wellcome Trust (206369/Z/17/Z).

453 **AUTHORS CONTRIBUTION**

454 Experiments were performed by MJL, HW, HDW and AD. SP, RPG, LS and GN  
455 collected, sequenced and isolated clinical viral isolates. MP, AHP, GDL, VMC, WF,  
456 NS, and RO generated reverse genetics-derived viruses. MJL, HW, HDW and AD  
457 analysed data. CMS provided reagents, funding support and advice. HW, MJL and  
458 SJDN analysed the data and wrote the manuscript. All authors edited the manuscript  
459 and provided comments.

460

461 **REFERENCES**

462

463 Bailey, C.C., Zhong, G., Huang, I.C., and Farzan, M. (2014). IFITM-Family Proteins: The Cell's  
464 First Line of Antiviral Defense. *Annu Rev Virol* **1**, 261-283.

465 Braun, E., Hotter, D., Koepke, L., Zech, F., Gross, R., Sparrer, K.M.J., Muller, J.A., Pfaller, C.K.,  
466 Heusinger, E., Wombacher, R., *et al.* (2019). Guanylate-Binding Proteins 2 and 5 Exert Broad  
467 Antiviral Activity by Inhibiting Furin-Mediated Processing of Viral Envelope Proteins. *Cell Rep*  
468 **27**, 2092-2104 e2010.

469 Brown, J.C., Goldhill, D.H., Zhou, J., Peacock, T.P., Frise, R., Goonawardane, N., Baillon, L.,  
470 Kugathasan, R., Pinto, A.L., McKay, P.F., *et al.* (2021). Increased transmission of SARS-CoV-2  
471 lineage B.1.1.7 (VOC 202012/01) is not accounted for by a replicative advantage in primary  
472 airway cells or antibody escape. *bioRxiv*, 2021.2002.2024.432576.

473 Chi, X., Yan, R., Zhang, J., Zhang, G., Zhang, Y., Hao, M., Zhang, Z., Fan, P., Dong, Y., Yang, Y.,  
474 *et al.* (2020). A neutralizing human antibody binds to the N-terminal domain of the Spike  
475 protein of SARS-CoV-2. *Science* **369**, 650-655.

476 Corey, L., Beyrer, C., Cohen, M.S., Michael, N.L., Bedford, T., and Rolland, M. (2021). SARS-  
477 CoV-2 Variants in Patients with Immunosuppression. *N Engl J Med* **385**, 562-566.

478 da Silva Filipe, A., Shepherd, J.G., Williams, T., Hughes, J., Aranday-Cortes, E., Asamaphan,  
479 P., Ashraf, S., Balcazar, C., Brunker, K., Campbell, A., *et al.* (2021). Genomic epidemiology  
480 reveals multiple introductions of SARS-CoV-2 from mainland Europe into Scotland. *Nat*  
481 *Microbiol* **6**, 112-122.

482 Fenton-May, A.E., Dibben, O., Emmerich, T., Ding, H., Pfafferott, K., Aasa-Chapman, M.M.,  
483 Pellegrino, P., Williams, I., Cohen, M.S., Gao, F., *et al.* (2013). Relative resistance of HIV-1  
484 founder viruses to control by interferon-alpha. *Retrovirology* **10**, 146.

485 Foster, T.L., Wilson, H., Iyer, S.S., Coss, K., Doores, K., Smith, S., Kellam, P., Finzi, A., Borrow,  
486 P., Hahn, B.H., *et al.* (2016). Resistance of Transmitted Founder HIV-1 to IFITM-Mediated  
487 Restriction. *Cell Host Microbe* *20*, 429-442.

488 Gaida, A., Becker, M.M., Schmid, C.D., Buhlmann, T., Louis, E.J., and Beck, H.P. (2011).  
489 Cloning of the repertoire of individual Plasmodium falciparum var genes using  
490 transformation associated recombination (TAR). *PLoS One* *6*, e17782.

491 Graham, C., Seow, J., Huettner, I., Khan, H., Kouphou, N., Acors, S., Winstone, H., Pickering,  
492 S., Galao, R.P., Dupont, L., *et al.* (2021). Neutralization potency of monoclonal antibodies  
493 recognizing dominant and subdominant epitopes on SARS-CoV-2 Spike is impacted by the  
494 B.1.1.7 variant. *Immunity* *54*, 1276-1289 e1276.

495 Guo, K., Barrett, B.S., Mickens, K.L., Hasenkrug, K.J., and Santiago, M.L. (2021). Interferon  
496 Resistance of Emerging SARS-CoV-2 Variants. *bioRxiv*.

497 Hoffmann, M., Kleine-Weber, H., and Pohlmann, S. (2020). A Multibasic Cleavage Site in the  
498 Spike Protein of SARS-CoV-2 Is Essential for Infection of Human Lung Cells. *Mol Cell* *78*, 779-  
499 784 e775.

500 Jia, R., Pan, Q., Ding, S., Rong, L., Liu, S.L., Geng, Y., Qiao, W., and Liang, C. (2012). The N-  
501 terminal region of IFITM3 modulates its antiviral activity by regulating IFITM3 cellular  
502 localization. *J Virol* *86*, 13697-13707.

503 Jia, R., Xu, F., Qian, J., Yao, Y., Miao, C., Zheng, Y.M., Liu, S.L., Guo, F., Geng, Y., Qiao, W., *et*  
504 *al.* (2014). Identification of an endocytic signal essential for the antiviral action of IFITM3.  
505 *Cell Microbiol* *16*, 1080-1093.

506 Jouvenet, N.G., C.; Banerjee, A. (2021). Clash of the titans: interferons and SARS-CoV-2.  
507 *Trends in Immunology*.

508 Kemp, S.A., Collier, D.A., Datir, R.P., Ferreira, I., Gayed, S., Jahun, A., Hosmillo, M., Rees-  
509 Spear, C., Mlcochova, P., Lumb, I.U., *et al.* (2021). SARS-CoV-2 evolution during treatment of  
510 chronic infection. *Nature* 592, 277-282.

511 Lindstrom, J.C., Engebretsen, S., Kristoffersen, A.B., Ro, G.O.I., Palomares, A.D., Engo-  
512 Monsen, K., Madslie, E.H., Forland, F., Nygard, K.M., Hagen, F., *et al.* (2021). Increased  
513 transmissibility of the alpha SARS-CoV-2 variant: evidence from contact tracing data in Oslo,  
514 January to February 2021. *Infect Dis (Lond)*, 1-6.

515 Liu, Y., Liu, J., Johnson, B.A., Xia, H., Ku, Z., Schindewolf, C., Widen, S.G., An, Z., Weaver, S.C.,  
516 Menachery, V.D., *et al.* (2021). Delta spike P681R mutation enhances SARS-CoV-2 fitness  
517 over Alpha variant. *bioRxiv*.

518 Mahase, E. (2021). Covid-19: Novavax vaccine efficacy is 86% against UK variant and 60%  
519 against South African variant. *BMJ* 372, n296.

520 Meng, B., Kemp, S.A., Papa, G., Datir, R., Ferreira, I., Marelli, S., Harvey, W.T., Lytras, S.,  
521 Mohamed, A., Gallo, G., *et al.* (2021). Recurrent emergence of SARS-CoV-2 spike deletion  
522 H69/V70 and its role in the Alpha variant B.1.1.7. *Cell Rep* 35, 109292.

523 Michael Rajah, M., Hubert, M., Bishop, E., Saunders, N., Robinot, R., Grzelak, L., Planas, D.,  
524 Dufloo, J., Gellenoncourt, S., Bongers, A., *et al.* (2021). SARS-CoV-2 Alpha, Beta and Delta  
525 variants display enhanced Spike-mediated Syncytia Formation. *EMBO J*, e108944.

526 Mohammad, A., Abubaker, J., and Al-Mulla, F. (2021). Structural modelling of SARS-CoV-2  
527 alpha variant (B.1.1.7) suggests enhanced furin binding and infectivity. *Virus Res* 303,  
528 198522.

529 Mok, B.W., Liu, H., Deng, S., Liu, J., Zhang, A.J., Lau, S.Y., Liu, S., Tam, R.C., Cremin, C.J., Ng,  
530 T.T., *et al.* (2021). Low dose inocula of SARS-CoV-2 Alpha variant transmits more efficiently  
531 than earlier variants in hamsters. *Commun Biol* 4, 1102.

532 Peacock, T.P., Goldhill, D.H., Zhou, J., Baillon, L., Frise, R., Swann, O.C., Kugathasan, R., Penn,  
533 R., Brown, J.C., Sanchez-David, R.Y., *et al.* (2021a). The furin cleavage site in the SARS-CoV-2  
534 spike protein is required for transmission in ferrets. *Nat Microbiol* 6, 899-909.

535 Peacock, T.P., Sheppard, C.M., Brown, J.C., Goonawardane, N., Zhou, J., Whiteley, M.,  
536 Consortium, P.V., de Silva, T.I., and Barclay, W.S. (2021b). The SARS-CoV-2 variants  
537 associated with infections in India, B.1.617, show enhanced spike cleavage by furin. *bioRxiv*,  
538 2021.2005.2028.446163.

539 Petrillo, C., Thorne, L.G., Unali, G., Schirolli, G., Giordano, A.M.S., Piras, F., Cuccovillo, I., Petit,  
540 S.J., Ahsan, F., Noursadeghi, M., *et al.* (2018). Cyclosporine H Overcomes Innate Immune  
541 Restrictions to Improve Lentiviral Transduction and Gene Editing In Human Hematopoietic  
542 Stem Cells. *Cell Stem Cell* 23, 820-832 e829.

543 Pickering, S., Batra, R., Merrick, B., Snell, L.B., Nebbia, G., Douthwaite, S., Reid, F., Patel, A.,  
544 Kia Ik, M.T., Patel, B., *et al.* (2021). Comparative performance of SARS-CoV-2 lateral flow  
545 antigen tests and association with detection of infectious virus in clinical specimens: a  
546 single-centre laboratory evaluation study. *Lancet Microbe* 2, e461-e471.

547 Planas, D., Veyer, D., Baidaliuk, A., Staropoli, I., Guivel-Benhassine, F., Rajah, M.M.,  
548 Planchais, C., Porrot, F., Robillard, N., Puech, J., *et al.* (2021). Reduced sensitivity of SARS-  
549 CoV-2 variant Delta to antibody neutralization. *Nature* 596, 276-280.

550 Rihn, S.J., Merits, A., Bakshi, S., Turnbull, M.L., Wickenhagen, A., Alexander, A.J.T., Baillie, C.,  
551 Brennan, B., Brown, F., Brunker, K., *et al.* (2021). A plasmid DNA-launched SARS-CoV-2  
552 reverse genetics system and coronavirus toolkit for COVID-19 research. *PLoS Biol* 19,  
553 e3001091.

554 Sanches, P.R.S., Charlie-Silva, I., Braz, H.L.B., Bittar, C., Freitas Calmon, M., Rahal, P., and  
555 Cilli, E.M. (2021). Recent advances in SARS-CoV-2 Spike protein and RBD mutations



556 comparison between new variants Alpha (B.1.1.7, United Kingdom), Beta (B.1.351, South  
557 Africa), Gamma (P.1, Brazil) and Delta (B.1.617.2, India). *J Virus Erad* 7, 100054.

558 Shen, X., Tang, H., McDanal, C., Wagh, K., Fischer, W., Theiler, J., Yoon, H., Li, D., Haynes,  
559 B.F., Sanders, K.O., *et al.* (2021). SARS-CoV-2 variant B.1.1.7 is susceptible to neutralizing  
560 antibodies elicited by ancestral spike vaccines. *Cell Host Microbe* 29, 529-539 e523.

561 Shi, G., Kenney, A.D., Kudryashova, E., Zani, A., Zhang, L., Lai, K.K., Hall-Stoodley, L.,  
562 Robinson, R.T., Kudryashov, D.S., Compton, A.A., *et al.* (2021). Opposing activities of IFITM  
563 proteins in SARS-CoV-2 infection. *EMBO J* 40, e106501.

564 Shi, G., Schwartz, O., and Compton, A.A. (2017). More than meets the I: the diverse antiviral  
565 and cellular functions of interferon-induced transmembrane proteins. *Retrovirology* 14, 53.

566 Tanaka, H., Hirayama, A., Nagai, H., Shirai, C., Takahashi, Y., Shinomiya, H., Taniguchi, C., and  
567 Ogata, T. (2021). Increased Transmissibility of the SARS-CoV-2 Alpha Variant in a Japanese  
568 Population. *Int J Environ Res Public Health* 18.

569 Tartour, K., Appourchaux, R., Gaillard, J., Nguyen, X.N., Durand, S., Turpin, J., Beaumont, E.,  
570 Roch, E., Berger, G., Mahieux, R., *et al.* (2014). IFITM proteins are incorporated onto HIV-1  
571 virion particles and negatively imprint their infectivity. *Retrovirology* 11, 103.

572 Thi Nhu Thao, T., Labroussaa, F., Ebert, N., V'Kovski, P., Stalder, H., Portmann, J., Kelly, J.,  
573 Steiner, S., Holwerda, M., Kratzel, A., *et al.* (2020). Rapid reconstruction of SARS-CoV-2 using  
574 a synthetic genomics platform. *Nature* 582, 561-565.

575 Thorne, L.G., Bouhaddou, M., Reuschl, A.K., Zuliani-Alvarez, L., Polacco, B., Pelin, A., Batra,  
576 J., Whelan, M.V.X., Ummadi, M., Rojic, A., *et al.* (2021). Evolution of enhanced innate  
577 immune evasion by the SARS-CoV-2 B.1.1.7 UK variant. *bioRxiv*.

578 Winstone, H., Lista, M.J., Reid, A.C., Bouton, C., Pickering, S., Galao, R.P., Kerridge, C.,  
579 Doores, K.J., Swanson, C.M., and Neil, S.J.D. (2021). The Polybasic Cleavage Site in SARS-  
580 CoV-2 Spike Modulates Viral Sensitivity to Type I Interferon and IFITM2. *J Virol* 95.  
581 Zhang, L., Mann, M., Syed, Z., Reynolds, H.M., Tian, E., Samara, N.L., Zeldin, D.C., Tabak, L.A.,  
582 and Ten Hagen, K.G. (2021). Furin cleavage of the SARS-CoV-2 spike is modulated by O-  
583 glycosylation. *bioRxiv*.  
584 Zhou, D., Dejnirattisai, W., Supasa, P., Liu, C., Mentzer, A.J., Ginn, H.M., Zhao, Y.,  
585 Duyvesteyn, H.M.E., Tuekprakhon, A., Nutalai, R., *et al.* (2021). Evidence of escape of SARS-  
586 CoV-2 variant B.1.351 from natural and vaccine-induced sera. *Cell* 184, 2348-2361 e2346.  
587  
588  
589  
590  
591  
592  
593  
594  
595

596 **FIGURE LEGENDS**

597 **Figure 1. IFITM sensitivity of SARS-CoV-2 variants of concern.** A) Schematic of  
598 Spike protein domains of the different variants of concern relative to the original  
599 Wuhan Spike sequence: alpha, beta, gamma and delta. The different mutations  
600 between the variants are represented in red. B-G) IFITM sensitivity of Wuhan,  
601 D614G, alpha, beta, gamma and delta PLVs in A549-ACE2 cells stably expressing  
602 the individual IFITMs. PLV entry was quantified by Luciferase activity 48 hours after  
603 infection and normalized to control cells. Data shown are mean  $\pm$  SEM, n=3.  
604 Statistics were calculated in Prism using *t*-test, stars indicate significance between  
605 control cell and individual IFITM (\*P=0.05).

606

607 **Figure 2. The alpha variant of SARS-CoV-2 is resistant to IFITMs.** A) D614G and  
608 Alpha PLVs infection of A549-ACE2 cells stably expressing the individual IFITMs.  
609 Infection was quantified by Luciferase activity 48 hours later and normalized to  
610 control cells. Data shown are mean  $\pm$  SEM, n=3. Statistics were calculated in Prism  
611 using *t*-test, stars indicate significance between control cell and individual IFITM  
612 (\*P=<0.05). B) Infection of A549-ACE2 stably expressing the individual IFITMs with  
613 England 02 and alpha full-length viruses at MOI 0.01. Infection was quantified by RT-  
614 qPCR of E gene relative to GAPDH 48 hours later; graph represents E mRNA levels  
615 relative to GAPDH. Data shown are mean  $\pm$  SEM, n=3. Statistics were calculated in  
616 Prism using *t*-test, stars indicate significance between control cell and individual  
617 IFITM (\*P=<0.05). C) Western blot from representative D614G and alpha PLVs  
618 produced in HEK293T/17 cells, and virions from full-length England-02 and alpha  
619 viruses. Virions were purified through a 20% sucrose gradient.

620

621 **Figure 3. The alpha variant is resistant to IFN $\beta$ .** A) England 02 and alpha full-  
622 length virus infection in A549-ACE2 cells pre-treated with IFN $\beta$ . Cells were pre-  
623 treated with increasing concentrations of IFN $\beta$  for 18 hours prior to infection with  
624 either virus at 500 E mRNA copies/cell. Infection was quantified by RT-qPCR of E  
625 mRNA from the supernatant 48 hours later and normalised to the un-treated control.  
626 Data shown are mean  $\pm$  SEM, n=3. Statistics were calculated in Prism using *t*-test,  
627 stars indicate significance between the different viruses at individual IFN  
628 concentrations (\*P=<0.05). B) England 02 and alpha full-length virus infection in  
629 Calu-3 cells pre-treated with IFN $\beta$ . Cells were pre-treated with increasing  
630 concentrations of IFN $\beta$  for 18 hours prior infection with either virus at 5000 E  
631 copies/cell. Infection was quantified by RT-qPCR of E mRNA from the supernatant  
632 48 hours later and normalised to the un-treated control. Data shown are mean  $\pm$   
633 SEM, n=3. Statistics were calculated in Prism using *t*-test, stars indicate  
634 significance between the different viruses at individual IFN concentrations  
635 (\*P=<0.05). C) England 02 and clinical isolates of alpha full-length virus infection in  
636 Calu-3 cells pre-treated with IFN $\beta$  and harvested as in A and B. Cells were pre-  
637 treated with increasing concentrations of IFN $\beta$  for 18 hours prior to infection with  
638 either virus at 5000 E copies/cell. Infection was quantified by RT-qPCR of cellular E  
639 mRNA relative to GAPDH 48 hours later and normalised to the un-treated control.  
640 Data shown are mean  $\pm$  SEM, n=3. Statistics were calculated in Prism using *t*-test,  
641 stars indicate significance between the different viruses at individual IFN  
642 concentrations (\*P=<0.05).

643

644 **Figure 4. The P681H mutation is necessary but not sufficient for IFITM**  
645 **resistance, and necessary and sufficient for IFN $\beta$  resistance.** A) D614G,

646 D614G- P681H, alpha, alpha- $\Delta$ HRRA, and alpha-H681P PLVs infection in A549-  
647 ACE2 cells stably expressing the individual IFITMs. PLVs entry was quantified by  
648 Luciferase activity 48 hours later and normalized to control cells. Data shown are  
649 mean  $\pm$  SEM, n=3. Statistics were calculated in Prism using t-test, black stars  
650 indicate significance relative to the control cells, red stars indicate significance  
651 between alpha and alpha-H681P in IFITM2 cells (\*P=<0.05). B) England 02 , alpha,  
652 and Wuhan-alpha Spike full-length virus infection in A549-ACE2 cells pre-treated  
653 with IFN $\beta$ . Cells were pre-treated with increasing concentrations of IFN $\beta$  for 18 hours  
654 prior to infection with either virus at 500 E copies/cell. Infection was quantified by RT-  
655 qPCR of E mRNA in the supernatant 48 hours later and normalised to the un-treated  
656 control. Data shown are mean  $\pm$  SEM, n=3. Statistics were calculated in Prism using  
657 t-test, stars indicate significance between the different viruses at individual IFN  
658 concentrations (\*P=<0.05). C) Wuhan(B.1.1.7 spike) and Wuhan(B1.1.7 spike  
659 H681P) Spike full-length virus infection in Calu-3 cells pre-treated with IFN $\beta$ . Cells  
660 were pre-treated with increasing concentrations of IFN $\beta$  for 18 hours prior to  
661 infection with either virus at 5000 E copies/cell. Infection was quantified by RT-qPCR  
662 of E mRNA in the supernatant 48 hours later and normalised to the un-treated  
663 control. Data shown are mean  $\pm$  SEM, n=3. Statistics were calculated in Prism using  
664 t-test, stars indicate significance between the different viruses at individual IFN  
665 concentrations (\*P=<0.05). D) A549-ACE2 cells were transfected with siRNAs  
666 against non-targeting control or IFITM2 for 24 hours and then treated with IFN $\beta$  for  
667 18 hours prior to infection with Wuhan(B.1.1.7 spike) or Wuhan(B.1.1.7 spike  
668 H681P) at 500 copies/cell. Infection was quantified by RT-qPCR of E gene relative to  
669 GAPDH 48 hours later; graph represents E mRNA levels relative to GAPDH. Data  
670 shown are mean  $\pm$  SEM, n=3. Statistics were calculated in Prism using t-test, stars

671 indicate significance between the different viruses at individual IFN concentrations  
672 (\* $P < 0.05$ ).

673

674 **Supplementary figure 1. Cyclosporin H treatment abolishes IFITM3**  
675 **enhancement of alpha PLVs.** A) D614G PLVs pre-treated with Cyclosporin H.  
676 A549-ACE2s stably expressing the individual IFITMs were pre-treated with 30  $\mu$ M of  
677 Cyclosporin H for 18 hours prior to infection with D614G PLVs. Infection was  
678 quantified by Luciferase activity 48 hours after infection and normalized to control  
679 cells. Data shown are mean  $\pm$  SEM,  $n=3$ . Statistics were calculated in Prism using  $t$ -  
680 test (\* $P < 0.05$ ). B) A549-ACE2s stably expressing the individual IFITMs were pre-  
681 treated with 30  $\mu$ M of Cyclosporin H for 18 hours prior to infection with alpha PLVs.  
682 Infection was quantified by Luciferase activity 48 hours after infection and normalized  
683 to control cells. Data shown are mean  $\pm$  SEM,  $n=3$ . Statistics were calculated in  
684 Prism using  $t$ -test, stars indicate significance between IFITM3 mock and IFITM3  
685 CsH (\* $P < 0.05$ ).

686

687 **Supplementary figure 2. alpha PLVs are less sensitive to inhibition by E64D**  
688 **than D614G PLVs.** A549-ACE2 cells were pre-treated with increasing  
689 concentrations of E64D for 1 hour prior infection with D614G or alpha PLVs. PLV  
690 entry was quantified by Luciferase activity 48 hours after infection and normalized to  
691 control cells. Data shown are mean  $\pm$  SEM,  $n=3$ .

692

693 **Supplementary figure 3. Spike processing of full-length virus and cleavage site**  
694 **PLVs mutants.** A) England-02, alpha, Wuhan(B.1.1.7 Spike), Wuhan(B.1.1.7 Spike  
695 H681P) were purified through 20% sucrose and immunoblotted for Spike and N

696 proteins. B) PLVs expressing different Spike mutants were produced in HEK293T-17  
697 cells and cell lysates and supernatant immunoblotted for gag and Spike. Supernatant  
698 was purified through 20% sucrose.

699

700 **Supplementary figure 4. IFITM sensitivity of individual alpha Spike mutations.**

701 A–F) PLVs with individual alpha mutations were used to infect A549-ACE2 cells  
702 stably expressing the individual IFITMs. Infection was quantified by Luciferase  
703 activity 48 hours after infection and normalized to control cells. Data shown are  
704 mean  $\pm$  SEM, n=3. Statistics were calculated in Prism using *t*-test, stars indicate  
705 significance between each PLVs control cell and individual IFITM (\*P=<0.05).

706

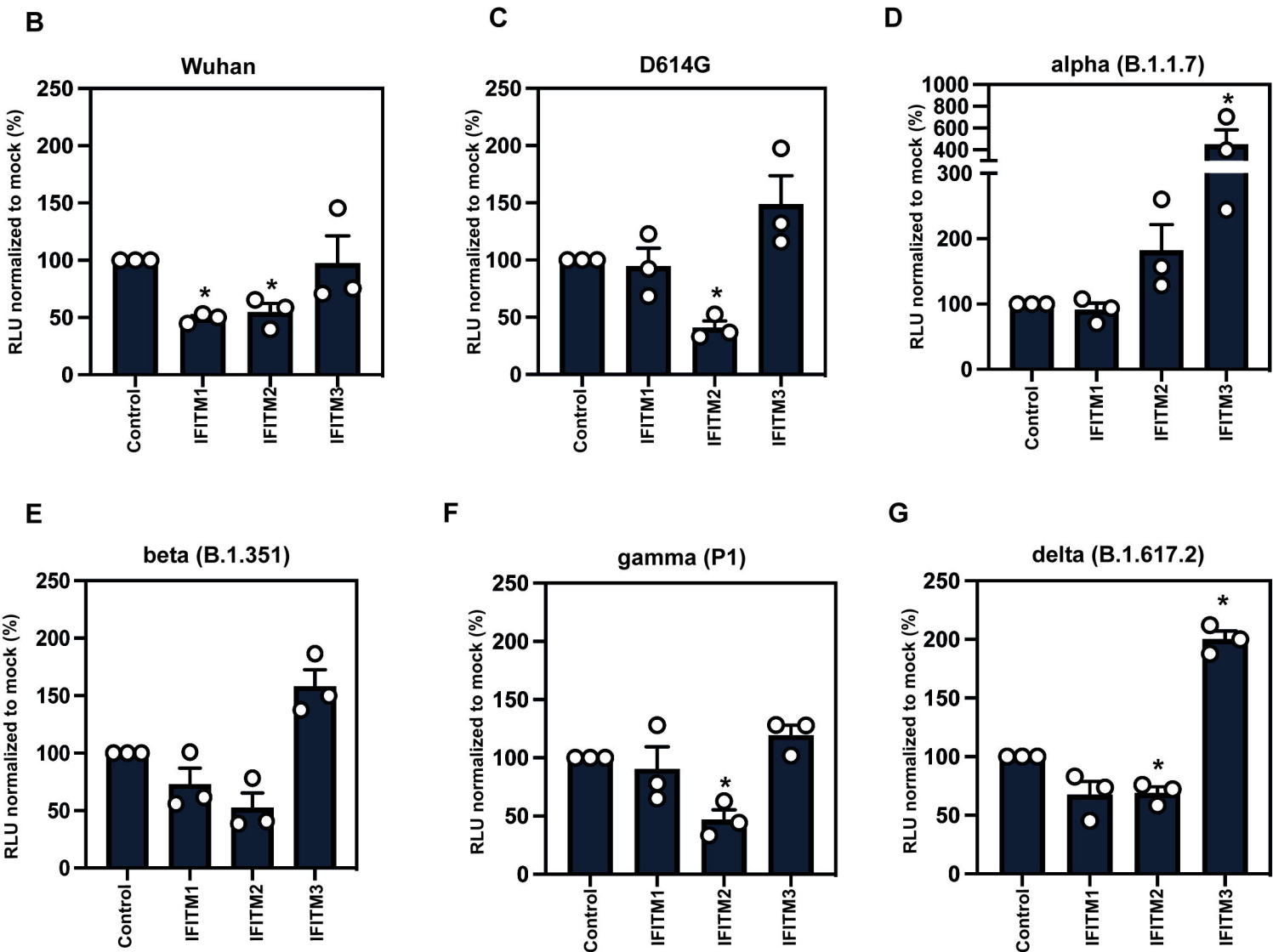
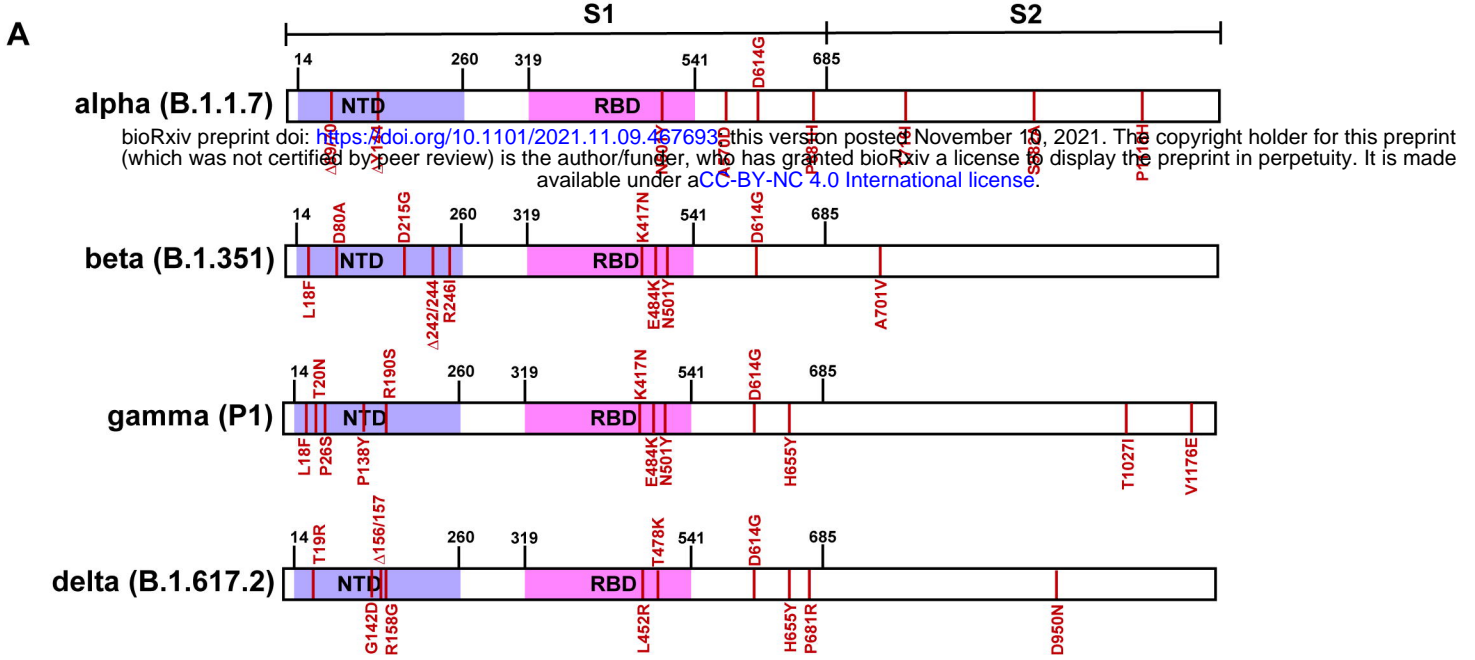


**Figure 1**



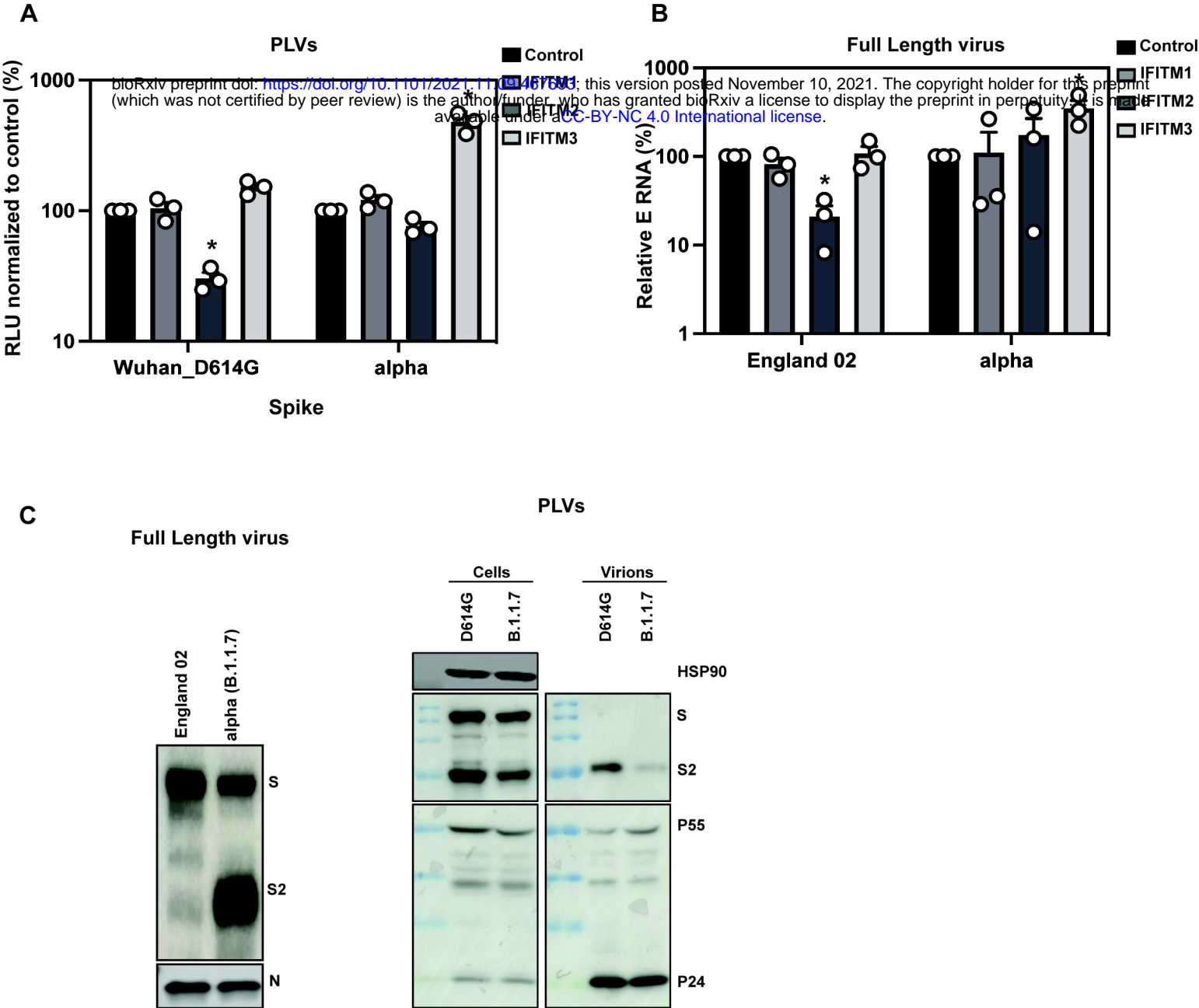


**Figure 2**

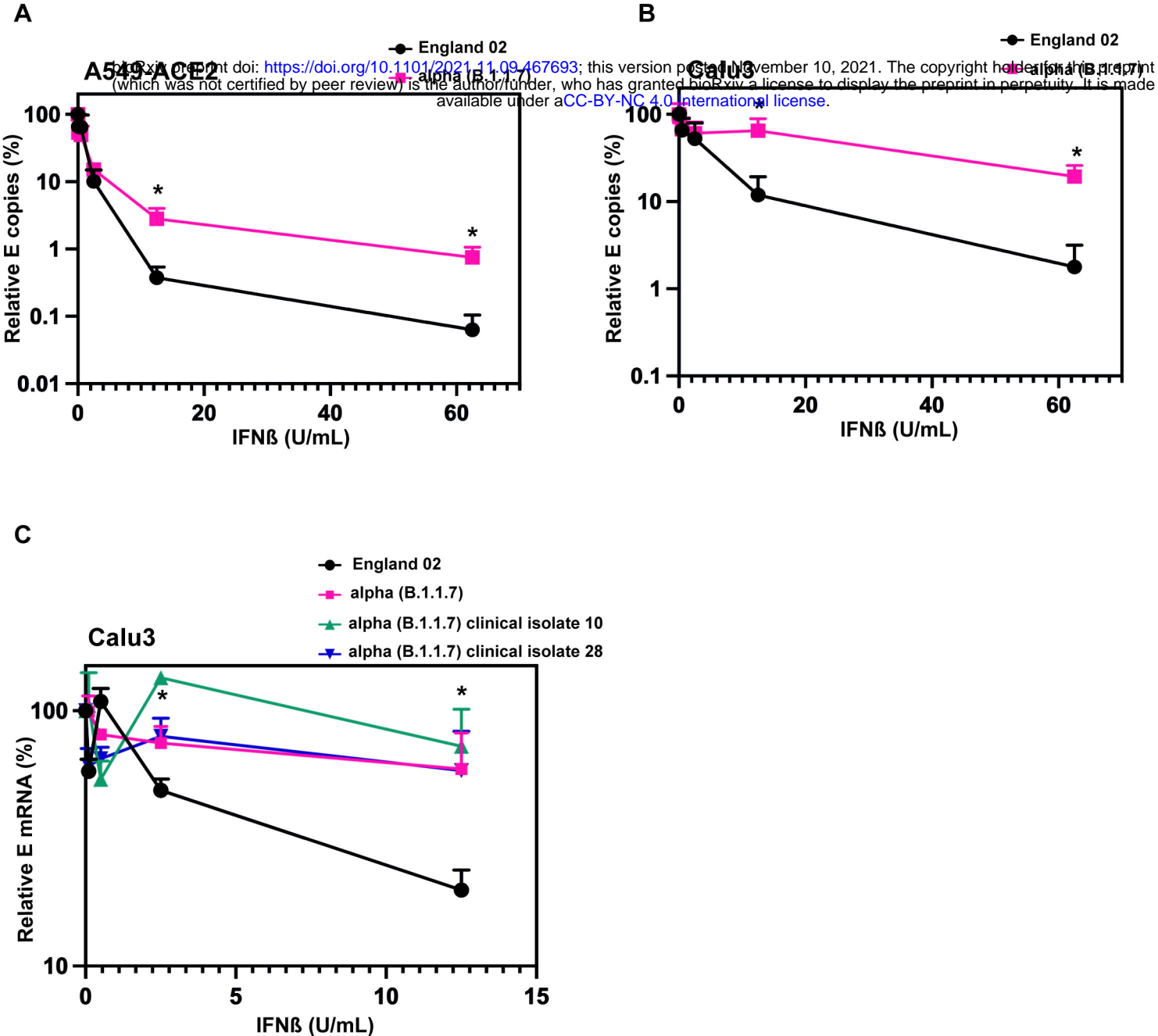
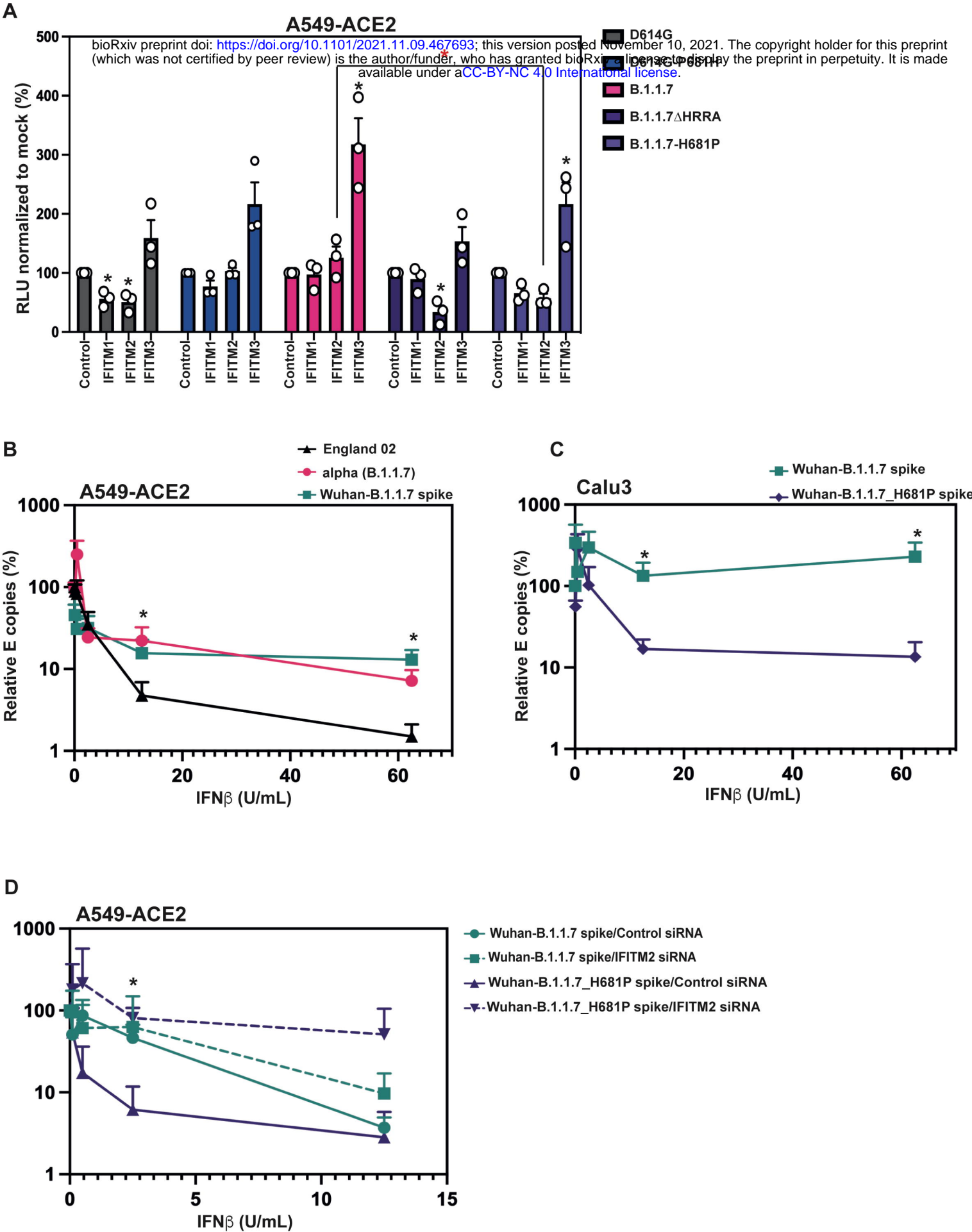
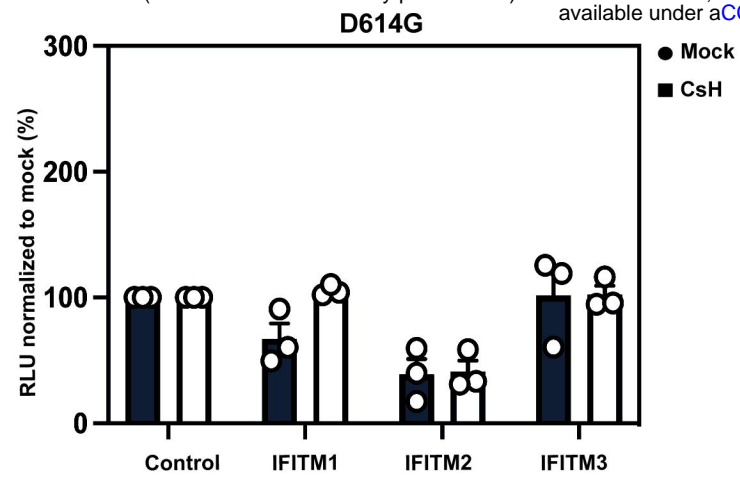


Figure 3

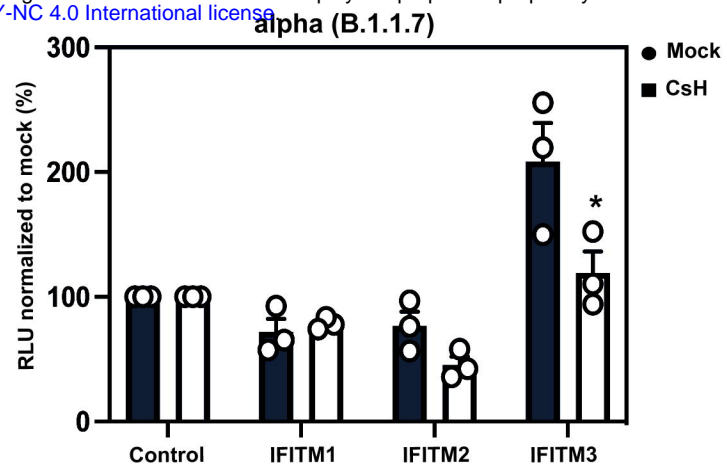


**Figure 4**

A

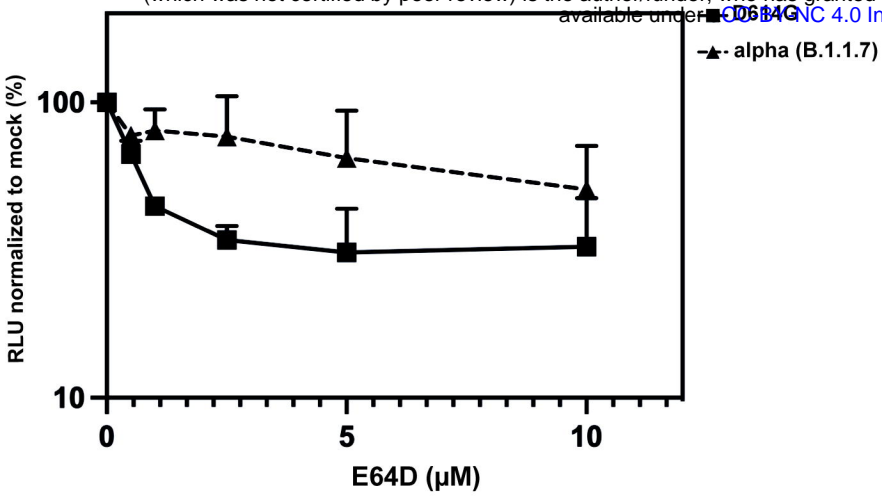


B



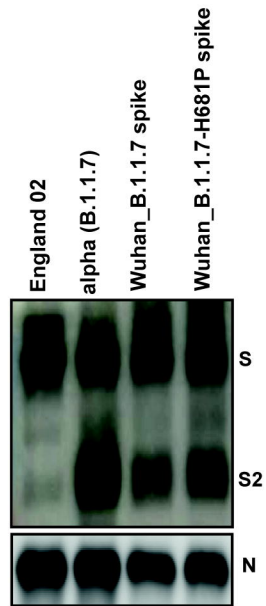
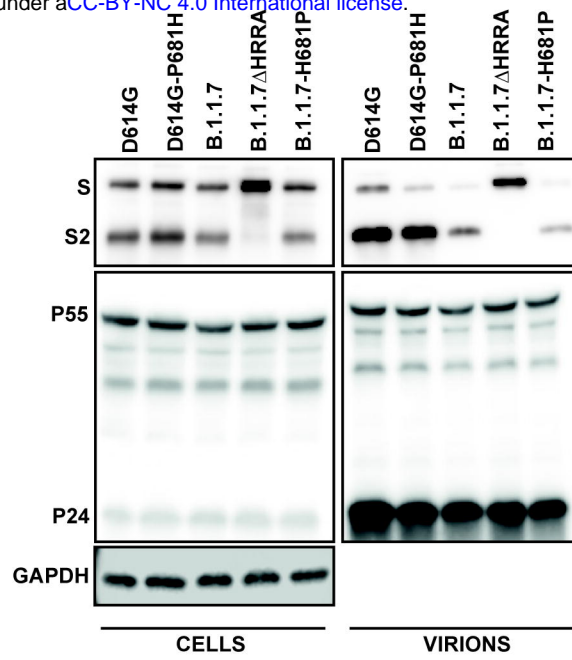
**A**

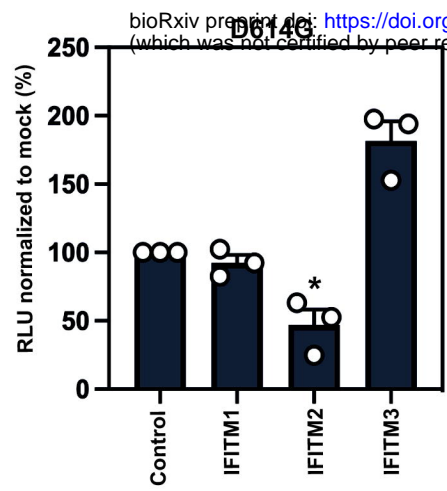
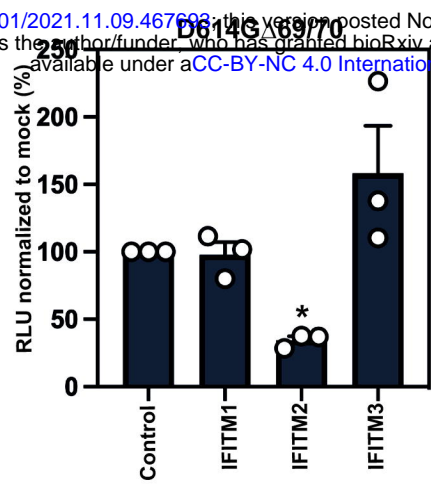
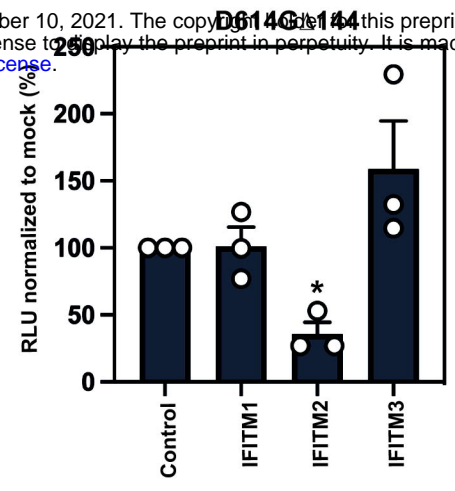
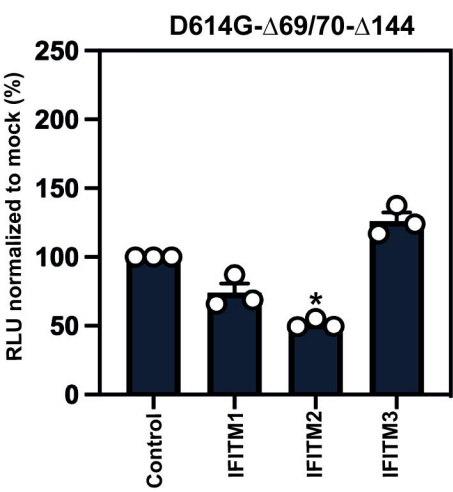
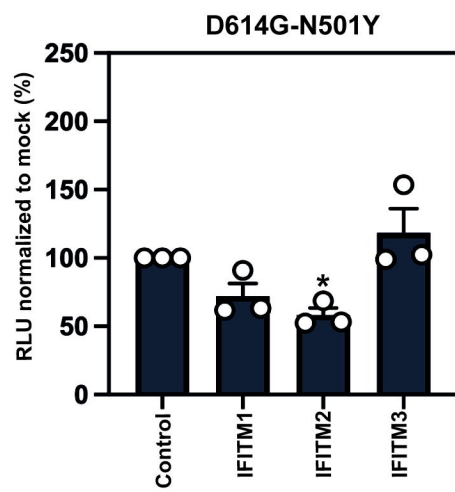
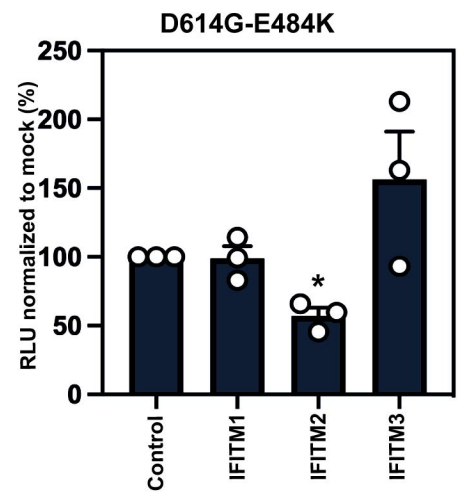
bioRxiv preprint doi: <https://doi.org/10.1101/2021.11.09.467693>; this version posted November 10, 2021. The copyright holder for this preprint (which was not certified by peer review) is the author/funder, who has granted bioRxiv a license to display the preprint in perpetuity. It is made available under aCC-BY-NC 4.0 International license.



**A**

bioRxiv preprint doi: <https://doi.org/10.1101/2021.11.09.467693>; this version posted November 10, 2021. The copyright holder for this preprint (which was not certified by peer review) is the author/funder, who has granted bioRxiv a license to display the preprint in perpetuity. It is made available under aCC-BY-NC 4.0 International license.

**B**

**A****B****C****D****E****F****G**